J. Mater. Environ. Sci. 7 (12) (2016) 4361-4374 *El Amraoui et al.*
ISSN : 2028-2508
CODEN: JMESCN

Bluff Body methane flame simulation: influence of turbulence modeling

R. El amraoui[*1], M. Mouqallid[2], H. El mghari[1], E. Affad[3], M. Obounou[4], D. Garreton[5]
1 Dep. Of physics Faculty of Science and Technics, Univ.Sultan MoulaySlimane, BéniMellal, Morocco
2Dep. Of energy, Ecole Nationale Supérieure des Arts et Métiers, Univ.MoulaySmail, Meknes, Morocco
3 Dep. Of physics, Faculty of Science and Technics, Univ. Hassan II, Mohammadia, Morocco
4 Dep. Of physics, Faculty of Science, Univ. of Yaoundé I, Yaoundé, Cameroun
5 EDF-DER-LNH, 6 Quai watier, Chatou, France

Received 28 Aug 2016, Revised 01 Oct 2016, Accepted 04 Oct 2016
**For correspondence: Email: r_amraoui64@yahoo.fr ; Phone: +212665669638; Fax: +212523485201*

Abstract
In turbulent combustion flows there is two phenomena namely turbulence and combustion. These two phenomena interact mutually. The turbulence causes fluctuations of all variables, however the combustion acts on the density and viscosity. In this paper we are interested in the study of the influence of the turbulence modeling on the characteristics of methane diffusion flame behind a bluff body obstacle, using the assumed probability density function with beta function for the estimation of the temperature and the mass fractions of species. The beta function parameters are the first and second moment of inert scalar.

Keywords : Turbulence modeling ; flame ; Turbulence chemistry interaction ; Bluff body burner

1. Introduction
The flow of bluff body has been widely investigated [1-7]. It is composed of two coaxial jets separated by an obstacle. The central jet is blocked or not depending on the report of the bulk velocities of the two streams. The experience shows the existence of one or two stagnation points on the axis of symmetry [5]. When the jet velocity increases, it enters further. In all cases a recirculation zone is generated behind the obstacle, it increases mixing between the fuel in the center and the air outside, and allows a better flame stability. The aerodynamics of this flow is complicated for two reasons: the first one is the curvature of the streamlines due to the existence of the recirculation zone. The second is the variation of the density consequent of the heat release. To better simulate the methane flame behind the bluff body, we will be interested in the study on the turbulence modeling and examine the improvement made by each of the three turbulence models considered. Averaged Favre is considered, thus all quantities are weighted by instantaneous density before averaging. The resulting equations are similar in form to the Reynolds equations for uniform density flow. The density variation terms are taken into account. The fast chemistry assumption is adopted. The temperature and the major species are calculated not by a transport equation but only by a presumed PDF model [8]. Beta function is used. It is calculated from the first two moments(mean and variance) of an inert scalar, whose are calculated from their transport equations. The dissipation of the scalar, fundamental variable for turbulent combustion models, is modeled using the proportionality assumption of dynamic to scalar time scales [9-10].

2. Governing equations
The instantaneous equations of momentum, mass and species are in principle sufficient to determine the aerodynamic state of the flow at any point and at any time. However chaotic and random nature of turbulence makes it difficult to obtain information from these equations. Then we decompose each quantity in a mean portion, and a fluctuating part. The latter contains information about the turbulent motion (energy and its dissipation).

The average value is defined as the result of an infinite number of experiences that have all the same initial and boundary conditions.
Due to the nonlinearity of the convection terms, the average procedure create new unknown terms, these are the correlation velocity - velocity and correlation scalar- velocity. The transport equation of these two correlations, in turn generate triple correlations. Thus we obtain an infinite hierarchy of equations. The closure problem is required, and consists to cut this chain at some level that determines the order of the model.
The average weighted by the mass or Favre average is used [11]. Indeed, it allows a simpler writing the balance equations. The following assumptions are valid:
• the gas mixture is assumed perfect
• the flow is low Mach number
• the fluids are Newtonian.

•The mass conservation equation is[12]:

$$\frac{\partial}{\partial t}\bar{\rho} + \frac{\partial}{\partial x_i}\bar{\rho}\widetilde{u_i} = 0 \quad (2.1)$$

Where $\bar{\rho}$is the mean density flow; $\widetilde{u_i}$ is the ith component of the velocity vector.

•The momentum conservation equationis[12]:

$$\frac{\partial}{\partial t}\bar{\rho}\widetilde{u_i} + \frac{\partial}{\partial x_j}\bar{\rho}\widetilde{u_i}\widetilde{u_j} = \frac{\partial}{\partial x_j}\left(\overline{\tau_{ij}} - \bar{\rho}\widetilde{u_i'' u_j''}\right) - \frac{\partial}{\partial x_i}\bar{p} + \bar{\rho}\widetilde{\gamma_i} \quad (2.2)$$

Where $\widetilde{\gamma_i}$ is a volume force.

The pressure is calculated by solving the Poisson equation obtained from equations (2.1) and (2.2)[13],and the density is calculated from the equation of state:

$$\frac{\bar{p}}{\bar{\rho}} = \frac{R\bar{T}}{M}$$

Where $\bar{T}$ is the temperature. It is calculated from a presumed pdf (section 2.4).
R is the gas constant, and M is the molar mass.

The composition of the inert scalar is calculated from the mixing rate, chemically inert scalar and whose transport equation is[12]:

$$\frac{\partial}{\partial t}\bar{\rho}\tilde{\theta} + \frac{\partial}{\partial x_i}\bar{\rho}\widetilde{u_i}\tilde{\theta} = -\frac{\partial}{\partial x_j}\left(\bar{J}_i^{\theta} + \bar{\rho}\widetilde{u_i'' \theta''}\right) (2.3)$$

$\overline{\tau_{ij}}$is the tensor of viscous stresses. For a Newtonian fluid, it can be connected to the strain tensor as[14]:

$$\overline{\tau_{ij}} = \mu\left(\frac{\partial \bar{u}_i}{\partial x_j} + \frac{\partial \bar{u}_j}{\partial x_i}\right) - \frac{2}{3}\mu\delta_{ij}\frac{\partial \bar{u}_k}{\partial x_k}$$

Whereδ_{ij} is the Kroneckersymbol.

$\bar{J}_i^{\theta}$ is the laminar diffusion flux ofθ. It is closed with a gradient law (Fick's law):

$$\bar{J}_i^{\theta} = -\bar{\rho}D_{\theta}\frac{\partial \bar{\theta}}{\partial x_i}$$

$D_{\theta}$is laminar diffusion coefficient of θ.

2.1 k-ε turbulence model

The Reynolds stresses and turbulent scalar flux are given by the gradients transport equations:

$$\widetilde{u_i'' u_j''} = -\nu_t \left(\frac{\partial \tilde{u}_i}{\partial x_j} + \frac{\partial \tilde{u}_j}{\partial x_i}\right) + \frac{2}{3}\delta_{ij}\,\tilde{k} + \frac{2}{3}\delta_{ij}\,\frac{\partial \tilde{u}_k}{\partial x_k}$$

$$\widetilde{u_i'' \theta''} = -\frac{\nu_t}{Sc_\theta}\frac{\partial \tilde{\theta}}{\partial x_i}$$

Where $\tilde{k}$ is the kinetic energy of turbulence;
Sc_θ is the turbulent Schmidt number. It is taken equal to 2/3.
ν_t is the coefficient of eddy viscosity. In the frame of the k-εmodel it is written:

$$\nu_t = C_\mu \frac{\tilde{k}^2}{\tilde{\varepsilon}}$$

$\tilde{k}$et$\tilde{\varepsilon}$ are calculated from the following transport equations:

$$\frac{\partial}{\partial t}\bar{\rho}\tilde{k} + \frac{\partial}{\partial x_i}\bar{\rho}\tilde{u}_i\tilde{k} = \frac{\partial}{\partial x_i}\left[\left(\mu + \frac{\mu_t}{\sigma_k}\right)\frac{\partial \tilde{k}}{\partial x_i}\right] + \bar{\rho}\widetilde{P_k} - \bar{\rho}\tilde{\varepsilon} - \frac{\nu_t}{\bar{\rho}}\frac{\partial \bar{\rho}}{\partial x_i}\frac{\partial \bar{p}}{\partial x_i} \quad (2.4)$$

$$\frac{\partial}{\partial t}\bar{\rho}\tilde{\varepsilon} + \frac{\partial}{\partial x_i}\bar{\rho}\tilde{u}_i\tilde{\varepsilon} = \frac{\partial}{\partial x_i}\left[\left(\mu + \frac{\mu_t}{\sigma_\varepsilon}\right)\frac{\partial \tilde{\varepsilon}}{\partial x_i}\right] + C_{\varepsilon 1}\bar{\rho}\frac{\tilde{\varepsilon}}{\tilde{k}}\left(\widetilde{P_k} - \frac{\nu_t}{\bar{\rho}^2}\frac{\partial \bar{\rho}}{\partial x_i}\frac{\partial \bar{p}}{\partial x_i}\right) - C_{\varepsilon 2}\bar{\rho}\frac{\tilde{\varepsilon}^2}{\tilde{k}} \quad (2.5)$$

Where :$\widetilde{P_k} = -\mu_t \frac{\partial \tilde{u}_i}{\partial x_j}\left(\frac{\partial \tilde{u}_i}{\partial x_j} + \frac{\partial \tilde{u}_j}{\partial x_i}\right) - \frac{2}{3}\tilde{k}\frac{\partial \tilde{u}_k}{\partial x_k} - \frac{2}{3}\mu_t\left(\frac{\partial \tilde{u}_k}{\partial x_k}\right)^2$

The constants of the k-ε model are given in the table 1below[12]:

C_μ	$C_{\varepsilon 1}$	$C_{\varepsilon 2}$	σ_k	σ_ε
0.09	1.44	1.92	1	1.3

Table 1: constants values of k-ε turbulence model

It should be noted that $\tilde{k}$ transport equation is derived from the Reynolds stresses ($\tilde{k}$=$\frac{1}{2}\widetilde{u_i'' u_i''}$). However, all terms of the dissipation transport equation are modeled.

2.2 Rij– ε turbulence model.

The Reynolds stress tensor is calculated by solving its transport equation. The following assumptions are made [12]:

• The Reynolds stress dissipation tensor is connected to the spherical tensor assuming local isotropy. Indeed, at high Reynolds numbers, smaller dissipative structures of the kinetic energy of turbulence are isotropic. Only normal stresses are dissipated and identically. It means that the dissipation tensor is related to kinetic energy dissipation rate as follows : $\varepsilon_{ij} = \frac{2}{3}\delta_{ij}\,\varepsilon$

• The term of pressure-strain correlation has two contributions; the first one is the interaction between the components of the fluctuating flow. Qualified by the return to isotropy, it is modeled by Rotta [15].
The second component is the interaction between the mean flow and the fluctuating flow. This contribution is called a quick part. Several closures have been proposed. We chose one of Naot et al. [16], also known as isotropisation of production.

• The diffusion of the Reynolds stresses by pressure fluctuations is negligible, whereas that by the turbulent flow is closed by means of the gradient hypothesis.

The source terms of the dissipation equation involve interactions at small scales and all require a closure. The first work on this equation is due to Davidov [17] and Harlow and Nakayama [18]. However they are Hanjalic and Launder [19] who proposed the first closed equation for dissipation, written in correspondence with the equation of k. In fact, ε is produced by the gradients of the mean velocity, and dissipated by viscosity effect. These two phenomena, production and dissipation are connected to those of the kinetic energy by means of the frequency of turbulence.

The equation for the dissipation proposed by Hanjalic and Launder [19]has been used successfully in various flow which are not too complicated. However, in the presence of complex phenomena such as recirculation, compression, swirl, .., several variants of this equation have been proposed to account for these phenomena.

The following equations are used for the Reynolds stresses and the kinetic energy dissipation rate:

$$\frac{\partial}{\partial t}\bar{\rho}\widetilde{u_i''u_j''} + \frac{\partial}{\partial x_k}\bar{\rho}\tilde{u}_k\widetilde{u_i''u_j''} = C_s\frac{\partial}{\partial x_m}\left(\bar{\rho}\frac{\tilde{k}}{\tilde{\varepsilon}}\widetilde{u_m''u_n''}\frac{\partial\widetilde{u_i''u_j''}}{\partial x_n}\right) - \bar{\rho}\widetilde{u_i''u_m''}\frac{\partial\tilde{u}_j}{\partial x_m} - \bar{\rho}\widetilde{u_j''u_m''}\frac{\partial\tilde{u}_i}{\partial x_m} - \frac{2}{3}\bar{\rho}\delta_{ij}\tilde{\varepsilon} - C_1\bar{\rho}\frac{\tilde{\varepsilon}}{\tilde{k}}\left(\widetilde{u_i''u_j''} - \frac{2}{3}\delta_{ij}\tilde{k}\right) - C_2\bar{\rho}\left(\tilde{P}_{ij} - \frac{2}{3}\delta_{ij}\tilde{P}_k\right) - \frac{\nu_t}{\bar{\rho}}\left[\frac{\partial\bar{\rho}}{\partial x_i}\frac{\partial\bar{p}}{\partial x_j} + \frac{\partial\bar{\rho}}{\partial x_j}\frac{\partial\bar{p}}{\partial x_i}\right] \quad (2.6)$$

Where : $\tilde{P}_{ij} = -\bar{\rho}\widetilde{u_i''u_m''}\frac{\partial\tilde{u}_j}{\partial x_m} - \bar{\rho}\widetilde{u_j''u_m''}\frac{\partial\tilde{u}_i}{\partial x_m}$ and $\tilde{P}_k = \frac{1}{2}\tilde{P}_{kk}$

$$\frac{\partial}{\partial t}\bar{\rho}\tilde{\varepsilon} + \frac{\partial}{\partial x_k}\bar{\rho}\tilde{u}_k\tilde{\varepsilon} = C_\varepsilon\frac{\partial}{\partial x_m}\left(\bar{\rho}\frac{\tilde{k}}{\tilde{\varepsilon}}\widetilde{u_m''u_n''}\frac{\partial\tilde{\varepsilon}}{\partial x_n}\right) - C_{\varepsilon1}\bar{\rho}\frac{\tilde{\varepsilon}}{\tilde{k}}\left(\widetilde{u_i''u_m''}\frac{\partial\tilde{u}_i}{\partial x_m} + \frac{\nu_t}{\bar{\rho}^2}\frac{\partial\bar{\rho}}{\partial x_i}\frac{\partial\bar{p}}{\partial x_i}\right) - C_{\varepsilon2}\bar{\rho}\frac{\tilde{\varepsilon}^2}{\tilde{k}} \quad (2.7)$$

The turbulent scalar flux is calculated according to the gradient hypothesis mentioned above (section 2.1).

2.3 Rij – Flux turbulence model.

The Reynolds stresses and turbulent scalar flux are derived from their balance equations. The assumptions mentioned above, and used when derived Reynolds stress equations, are again used in order to establish the scalar flux equation. The transport equations for $\widetilde{u_i''u_j''}$ and $\tilde{\varepsilon}$are (2.6) and (2.7) respectively and that of $\widetilde{u_i''\theta''}$ is as follows:

$$\frac{\partial}{\partial t}\bar{\rho}\,\widetilde{u_i''\theta''} + \frac{\partial}{\partial x_k}\bar{\rho}\tilde{u}_k\widetilde{u_i''\theta''} = C_{s\theta}\frac{\partial}{\partial x_m}\left(\bar{\rho}\frac{\tilde{k}}{\tilde{\varepsilon}}\widetilde{u_m''u_n''}\frac{\partial\widetilde{u_i''\theta''}}{\partial x_n}\right) - \bar{\rho}\widetilde{u_m''\theta''}\frac{\partial\tilde{u}_i}{\partial x_m} - \bar{\rho}\widetilde{u_i''u_m''}\frac{\partial\tilde{\theta}}{\partial x_m}$$
$$-C_{\theta1}\bar{\rho}\frac{\tilde{\varepsilon}}{\tilde{k}}\widetilde{u_i''\theta''} + C_{\theta2}\bar{\rho}\widetilde{u_m''\theta''}\frac{\partial\tilde{u}_i}{\partial x_m} \quad (2.8)$$

The constants of Rij – ε model–and Rij – Flux model are initially proposed by Launder et al.[20], and generalized to flows with swirl by Hogg and Leschziner [21] and Bel Hassan and Simonin [13]. They are given in the table 2 below:

C_1	C_2	$C_{\theta1}$	$C_{\theta2}$	C_s	C_ε	$C_{s\theta}$
1.8	0.6	3	0.5	0.22	0.18	0.18

Table 2: Constants of Rij – ε model –and Rij – Flux model

2.4 Turbulent combustion modeling

The objective of this study is not to study a detailed simulation of the chemical kinetics of methane flame, we simply represent it by a single chemical reaction in order to calculate the heat release and the major species.

The following assumptions are made:

Fast chemistry assumption
The Lewis number is equal to 1
The number of Damkholer is great.

Damkohler number is the ratio of flow time scale to reaction time scale. For large Damkohler number, i.e. short chemical time scale compared to dynamic time one, chemistry is fast, and reaction sheets of various wrinkled types may occur [22]. In this case, Attiti and al. [23] found that extinction is negligible in turbulent non premixed flames. However Sanchez and al.[24] in their study correlate the diminishing of Damkohler number and the instability of the flame.
The Lewis number $L_e$is the ratio of Schmidt number to Prandtl number, i.e. the ratio of thermal to mass diffusion. For many gases Lewis number is assumed to be of the order of 1 [22,25]. When Lewis number is nonunity, which means that mass and heat can diffuse at different rates, than a flame instability can occur [22]. More generally, the later situation, i.e. $L_e \neq 1$has enlightened several combustion mechanisms like stretched flames, local extinction, soot formation [26-28]. For more details on these combustion phenomena one can see Law [29].

The temperature and the chemical species are calculated from the probability density function P(θ):

$$\tilde{y}_i = \int_0^1 y_i(\theta) P(\theta) d\theta \quad (2.9)$$

Several forms of P(θ) have been proposed (Sinusoidal[30]; rectangles[8]; clipped Gaussian[31]; triangle [32]; …). We used the beta function proposed by Richardson [33]. It is based on the first two moments of an inert scalar (mean and variance). We have:

$$1 = \int_0^1 P(\theta) d\theta$$

$$\tilde{\theta} = \int_0^1 \theta P(\theta) d\theta$$

$$\widetilde{\theta''^2} = \int_0^1 \left(\theta - \tilde{\theta}\right)^2 P(\theta) d\theta$$

The probability density function is defined as :

$$P(\theta) = \frac{\theta^a (1-\theta)^b}{\gamma}$$

where a=z$\tilde{\theta}$-1 ; b=z(1-$\tilde{\theta}$)-1 and $\gamma = \int_0^1 \theta^{a+1}(1-\theta)^b d\theta$ with$z = \frac{\tilde{\theta}(1-\tilde{\theta})}{\widetilde{\theta''^2}} - 1$

The variance of the scalar is determined by its transport equation, which is written differently depending on whether the turbulent scalar flux is transported or not. Using Favre averaged, and after modeling turbulent diffusion, this equation becomes:

$$\frac{\partial}{\partial t}\bar{\rho}\widetilde{\theta''^2} + \frac{\partial}{\partial x_k}\bar{\rho}\widetilde{u_k}\widetilde{\theta''^2} = C_\theta \frac{\partial}{\partial x_m}\left(\bar{\rho}\frac{\tilde{k}}{\tilde{\varepsilon}}\widetilde{u_m''u_n''}\frac{\partial\widetilde{\theta''^2}}{\partial x_n}\right) - 2\bar{\rho}\widetilde{u_i''\theta''}\frac{\partial\tilde{\theta}}{\partial x_i} - 2\bar{\rho}\tilde{\varepsilon}_\theta \quad (2.10)$$

In the frame ofR_{ij} – Flux model, and

$$\frac{\partial}{\partial t}\bar{\rho}\widetilde{\theta''^2} + \frac{\partial}{\partial x_k}\bar{\rho}\widetilde{u_k}\widetilde{\theta''^2} = \frac{\partial}{\partial x_i}\left[\left(D_\theta + \frac{\mu_t}{Sc_{\theta 2}}\right)\frac{\partial\widetilde{\theta''^2}}{\partial x_i}\right] - 2\bar{\rho}\frac{\nu_t}{Sc_\theta}\left(\frac{\partial\tilde{\theta}}{\partial x_i}\right)^2 - 2\bar{\rho}\tilde{\varepsilon}_\theta \quad (2.11)$$

In the frame of k-ε andR_{ij}–ε models.

$\tilde{\varepsilon}_\theta$ is the scalar dissipation. It is defined as follows:

$$\tilde{\varepsilon}_\theta = D_\theta \frac{\partial \theta''}{\partial x_i}\frac{\partial \theta''}{\partial x_i}$$

C_θ and $Sc_{\theta 2}$ are constants. Their values are 0.18 and 2/3 respectively.

Two methods are possible for calculating $\tilde{\varepsilon}_\theta$. The first one is to solve the $\tilde{\varepsilon}_\theta$ transport equation; the second is to link the dynamic time scale and the scalar time scale. This assumption is due to Monin [9] We write :

$$\tau_\theta = r\tau_t \text{; where : } \tau_t = \frac{\overline{q^2}}{\tilde{\varepsilon}} \text{ and } \tau_\theta = \frac{\overline{\theta'^2}}{\tilde{\varepsilon}_\theta}.\overline{q^2} = 2\,\bar{k}$$

The establishing of proportionality constant r was the subject of many theoretical and experimental studies. Spalding [34] estimates that r is a universal constant and is equal to 0.5. Launder [35] proposes the value 0.8 in the case of homogeneous flows. Many experiences where done in the grid turbulence. They were synthesized by Warhaft and Lumley [36], they indicate the relative dispersion of values of r, and found $0.4 \leq r \leq 1.5$.
For our study we chose the value r = 0.8

3. Numerical method – test case description

3.1 Numerical method:

The strong nonlinearity of fluid mechanics equations coupled with those of turbulence models generate difficulty to search any analytical solution. We research numerical resolution; thus, we approximate the continuous real solution by a discontinuous solution in time and in space.
Here we have used the fractional step method [37]. It solves, instead of the differential equation of the total balance equation, simple differential equations type convection or diffusion. The spatial discretization is performed by the finite difference method, the time integration is conducted using a semi-implicit method of the first order. The mesh is two-dimensional orthogonal plane or axisymmetric. The various transported quantities are distributed on two staggered grids. The nodes of the first one, known as velocity mesh, are located the components of the velocity and the mean scalar. The nodes of the second grid, pressure mesh, are the points where the pressure, Reynolds stresses, turbulent scalar flux, the dissipation ....are calculated. The nodes of the second grid are in the center of the first one.

3.2 Test case description:

The Bluff Body flow is composed of a mixture of two concentric jets separated by a central body. The recirculation zone created behind the obstacle increases the efficiency of mixing of the two fluids, and consequently produces better flame stability in the reactive case. Many authors were interested in the case of bluff-body [38-40]. We chose here the case studied by Namazian, Schefer and Kelly at Sandia National Laboratories and Perrin of GDF[5]. The geometrical configuration is shown in the figure 1.

The central jet is a methane flow of a pipe of 750 mm in length and 5.4 mm in diameter. The flow velocity is 21 m/s, thus the Reynolds number is 7000 based on the diameter of the pipe. The flow is established at the outlet of the jet. The air is injected around the bluff body by an annular pipe whose inside diameter is D_b= 50mm and an external diameter D_e = 100mm. Upstream of the exit of aircoflow, are installed a honeycomb, and two grids plans to homogenize the flow, which leads to uniform mean axial velocity within 1%. The flow velocity of the annular air is 15m /s.

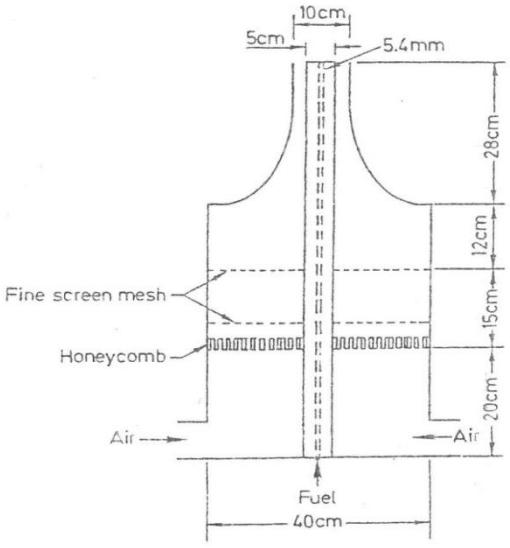

Figure 1: Schematic drawing of the bluff body stabilized flame[5].

4. Results and discussion

Computational domain- boundary conditions

The flow is axially symmetrical, only a radial plane is considered for calculation. A low-velocity air flow is added in order to allow the development and training of the annular air flow firstly, and secondly to minimize the influence of the boundary conditions on the main flow of the bluff body[41].
The boundary conditions are:

• radial gradients are set to zero on the axis of symmetry; moreover, the average radial velocity is equal to zero;
• axial gradients are set to zero at the exit for all variables except for the pressure, which is imposed;
• Slip conditions on the right (Figure 2);
• Classic wall laws, that is, logarithmic or linear velocity profile based on the value of y^+[42];
• Dirichlet condition at the inlets.

The mesh is not uniform in both directions of space. It is especially refined in the recirculation zone which exhibits high shear. The mesh size sensitivity test is performed, and 72x125 meshes are used for the computational domain. Thus the solution domain extends from de bluff body surface to 47 methane jet diameters in the axial direction and 37 methane jet diameters from de centerline in the radial direction.

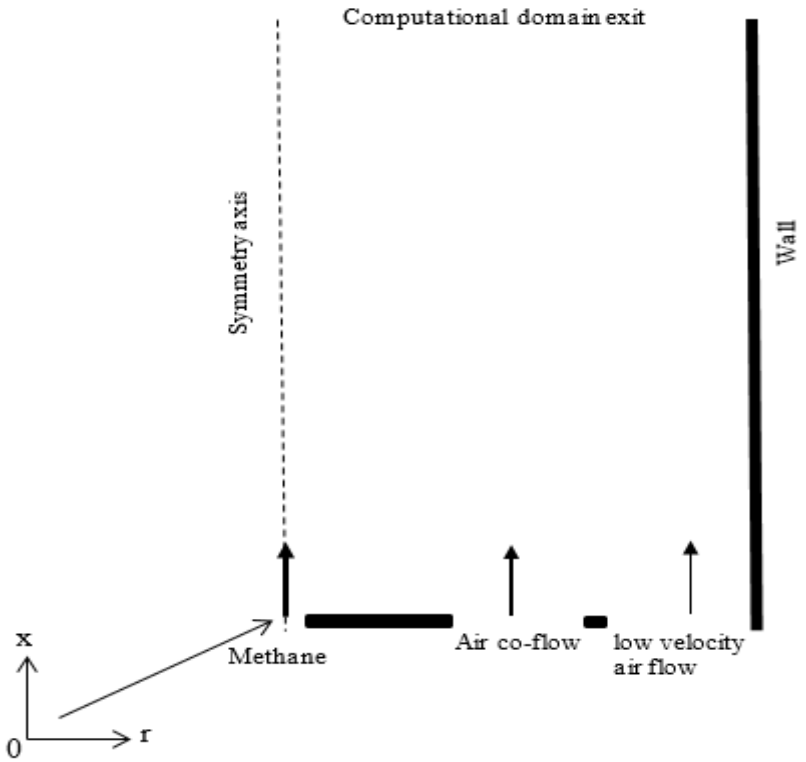

Figure 2 : Computationaldomain

The predictions of three models namely k-ε model, Rij-ε model and Rij-Flux model are compared to measurements. **Figure 3** shows the mean axial velocity profile at eight radial sections. The recirculation zone length is under-predicted by the three models. However the stagnation point location is well predicted (about 10 mm from the axis in radial direction) in accordance with the experience (see the radial evolution at x=60 mm). Up to x=70mm the mean axial velocity is under-predicted by k-ε model and R_{ij} – ε model. However the R_{ij} – Flux model predicts well the decay rate of the axial velocity.

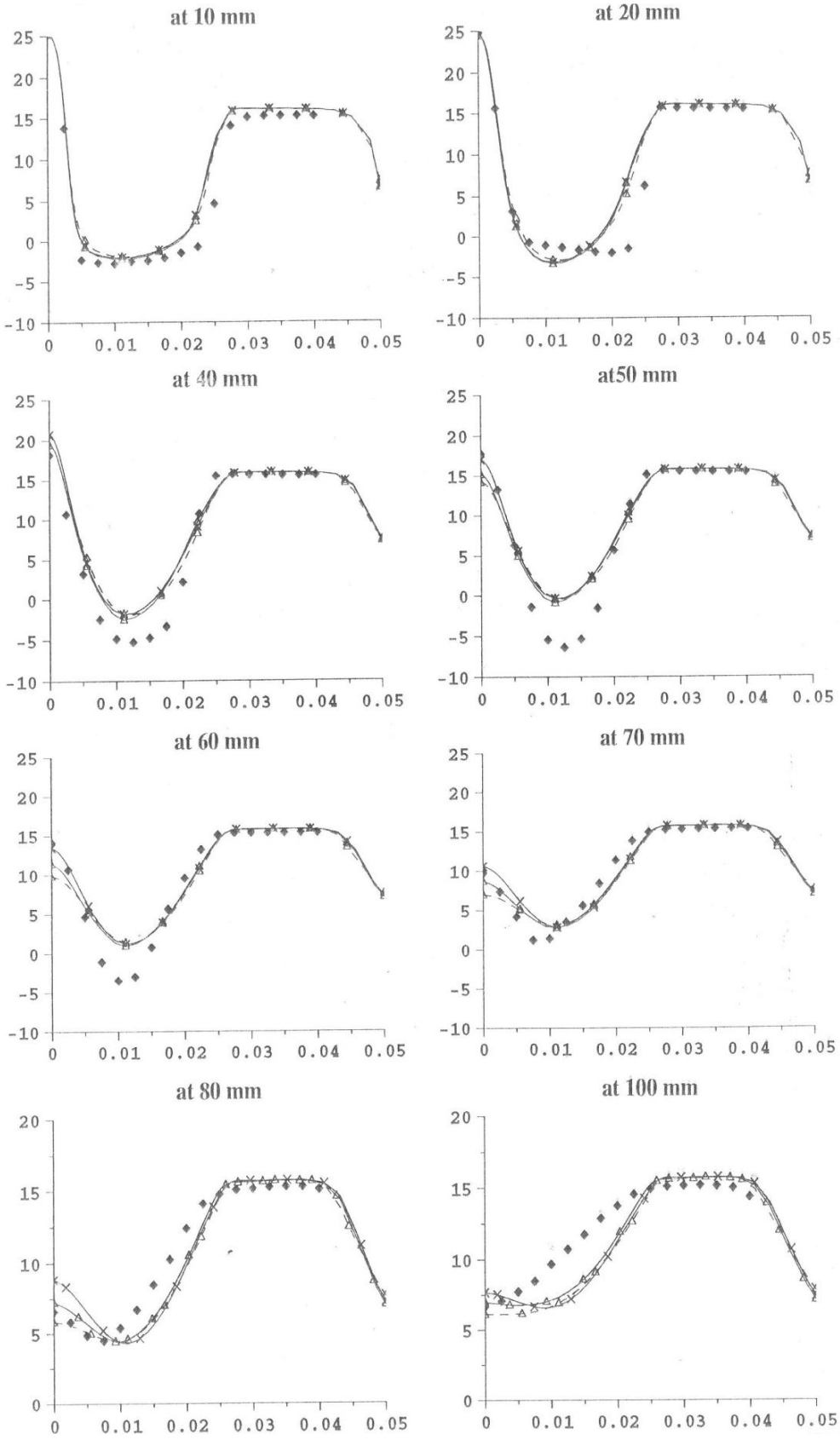

Figure 3 : radial profiles of mean axial velocity in $\frac{m}{s}$ at different axial locations.
Δ---Δ:k-ε ;ΔΔ:R_{ij} -ε ;xx: R_{ij}-Flux ;♦:experiment

At the recirculation zone, the radial mean velocity is minimum near the axis of symmetry (methane jet) and away from the axis of symmetry at air flow. It is maximum at both edges of the recirculation zone (**Figure 4**). This trend is predicted by the three models. However the mean radial velocity values in these two edges are underestimated.

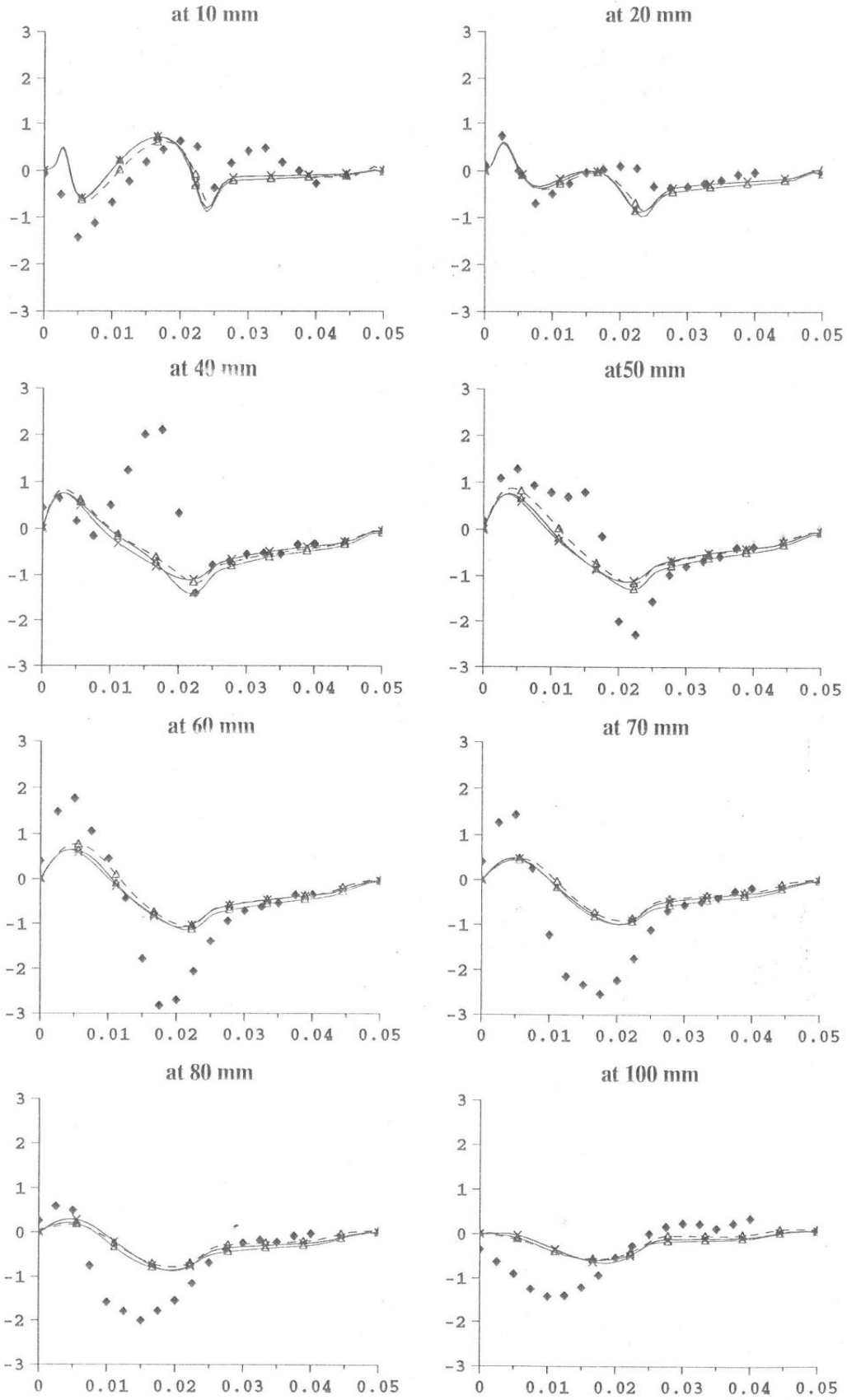

Figure 4 : radial profiles of mean radial velocity in $\frac{m}{s}$ at different axial locations.
∆---∆:k-ε ;∆∆:R_{ij}-ε ;xx: R_{ij}-Flux ;♦:experiment

The comparison of simulations and measurements of radial evolutions for rms fluctuation of the axial velocity and radial evolutions of rms fluctuation of the radial velocity are shown on **Figure 5** and **Figure 6** respectively. The following comments can be drawn:

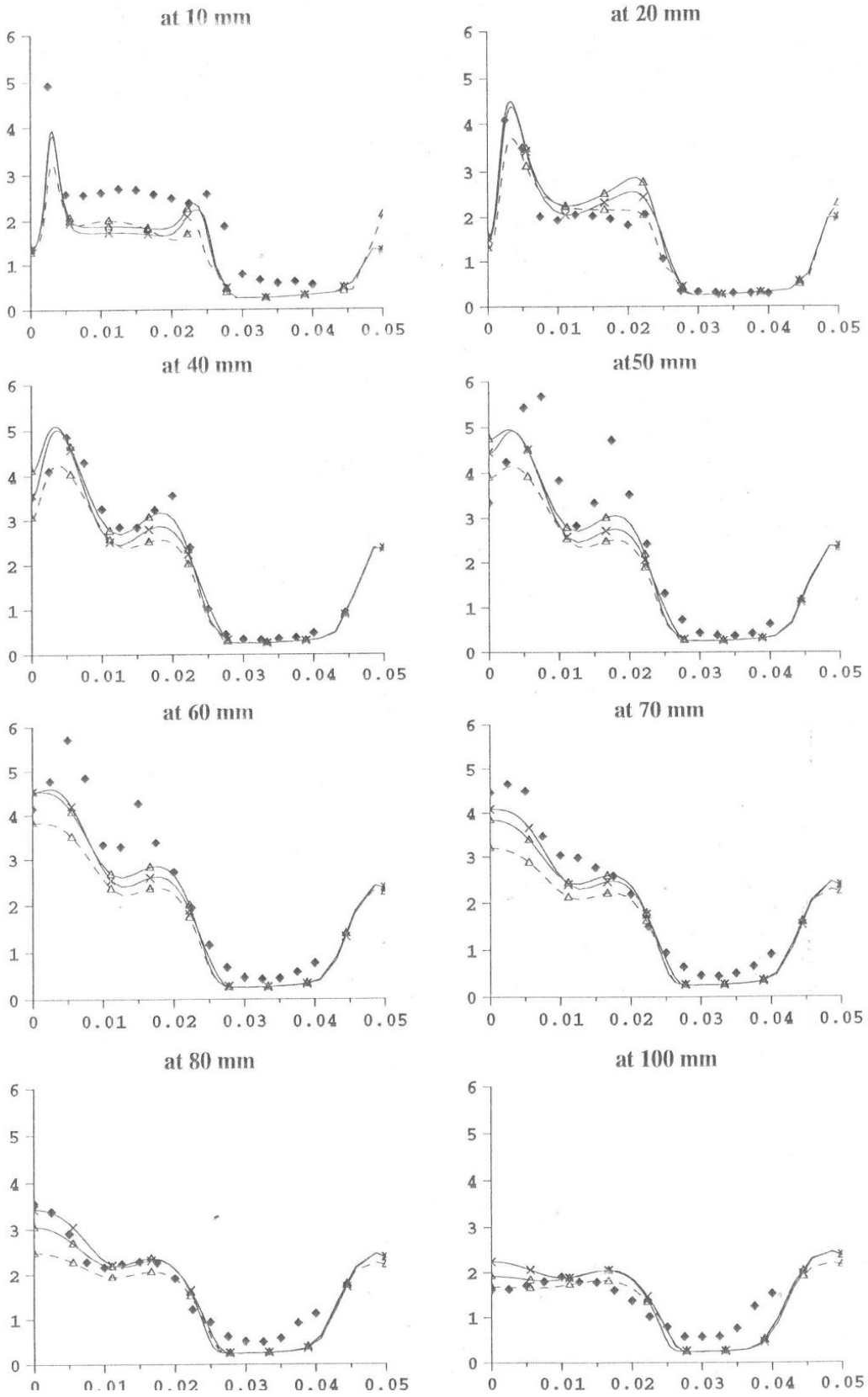

Figure 5 : radial profiles of rms of mean axial velocity at different axial locations. ∆---∆:k-ε ;∆∆:~~R_{ij} ε~~; x x: R_{ij}-F~~lux~~;♦:experiment

Velocity fluctuations pass through two peaks respectively at the two edges of the recirculation zone. This trend is predicted by all models. The k-ε model underestimates rms of axial velocity and overestimates rms of radial velocity in the recirculation zone. The anisotropy of the flow is correctly predicted by R_{ij}-ε and R_{ij} -Flux model, unlike k-ε, who gives roughly the same levels for both rms.

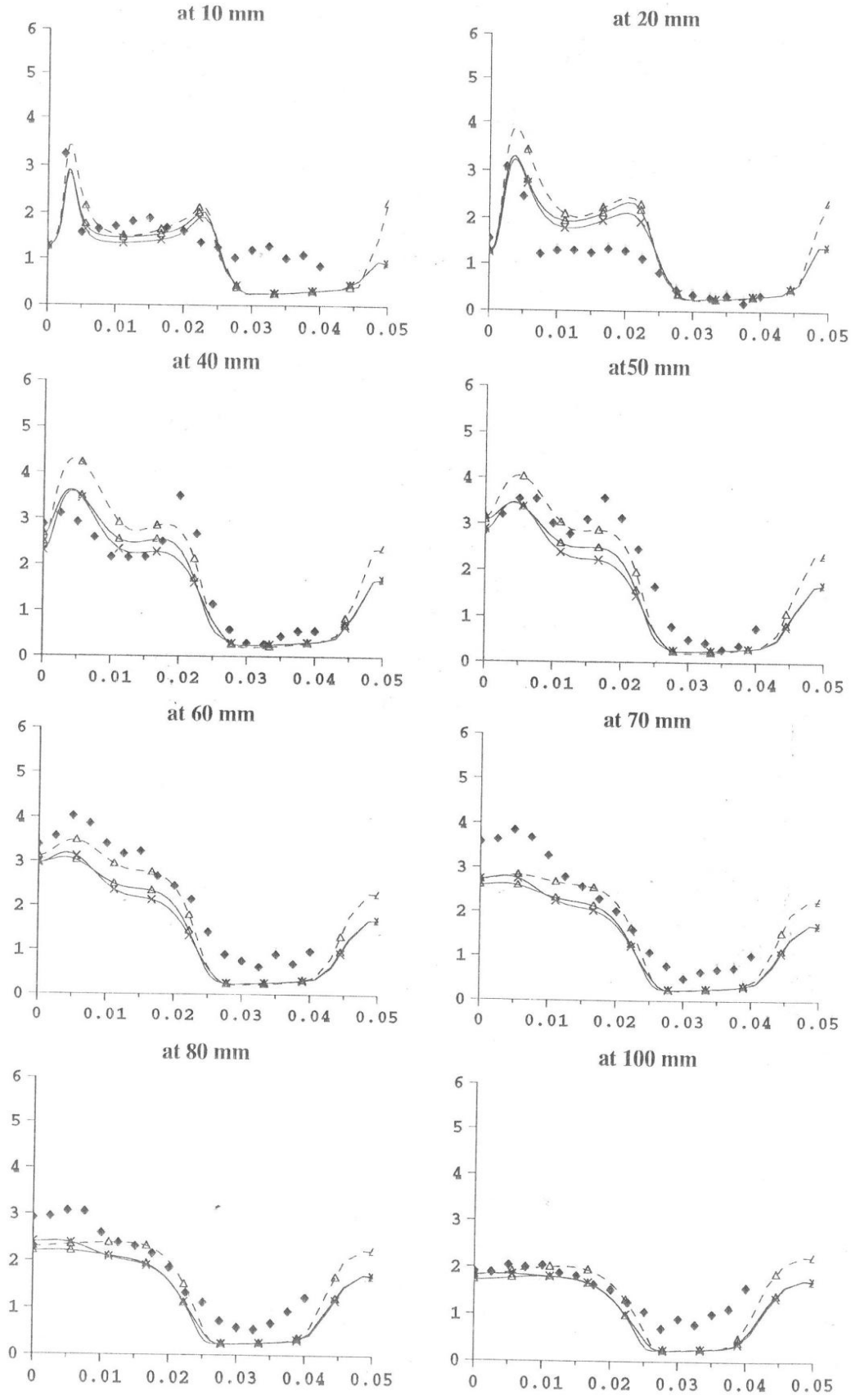

Figure 6 : radial profiles of rms of mean radial velocity at different axial locations.
Δ---Δ:k-ε ;ΔΔ:R_{ij}-ε; x x: R_{ij}-Flux ;♦:experiment

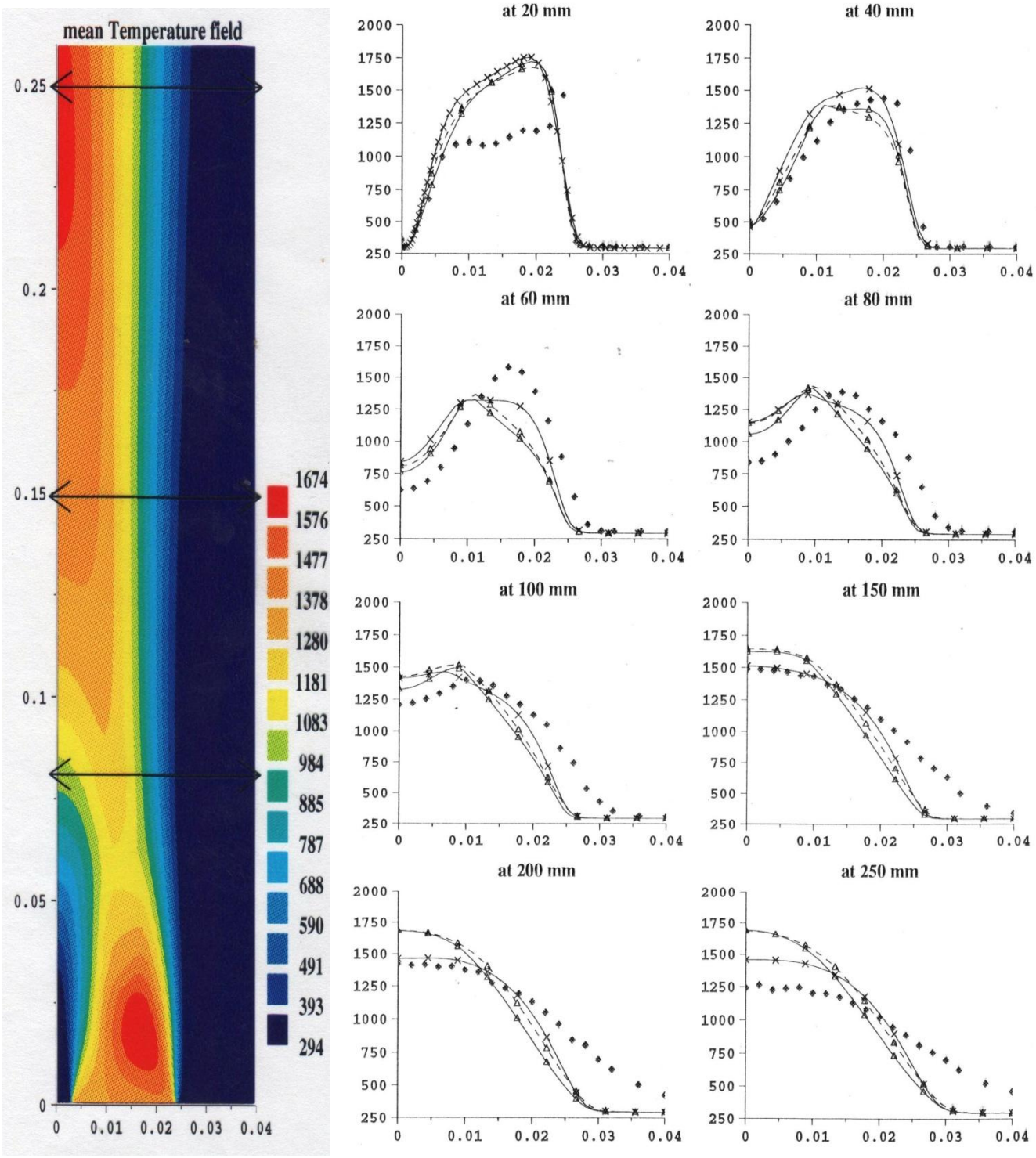

Figure 7 : the temperature field computed with R_{ij}-ε model (on the left) and the radial evolutions of the temperature (on the right) compared with the experiments.
Δ---Δ:k-ε ;ΔΔ:R_{ij}-ε ; x x: R_{ij}-Flux ;♦:experiment

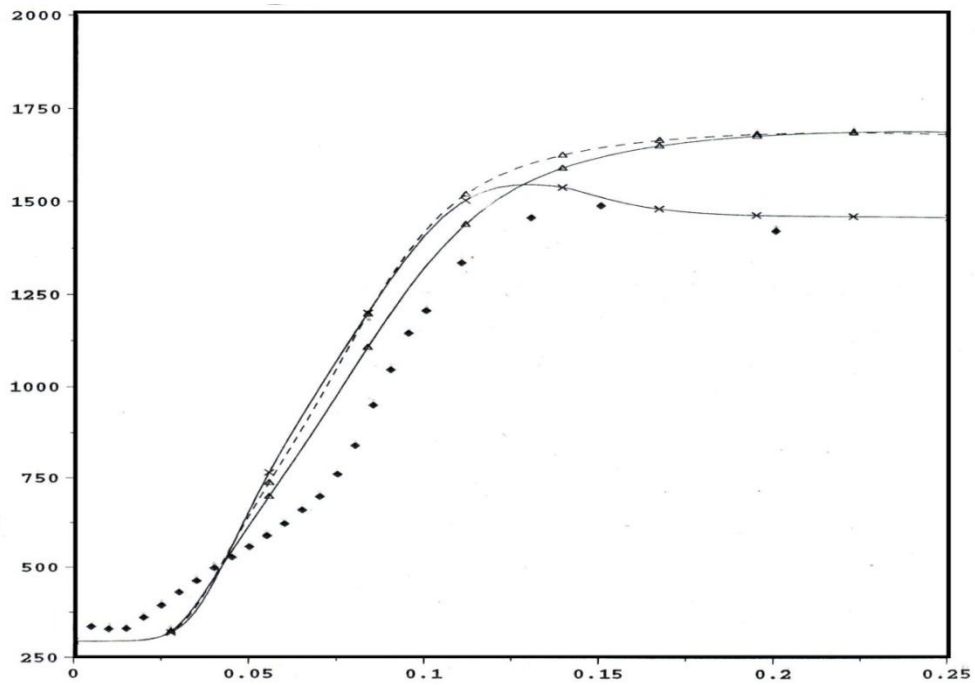

Figure 8 : the axial evolution of the temperature on the symmetry axis compared with the experiments.Δ---Δ:k-ε ;ΔΔ:R_{ij}-ε ; x x: R_{ij}-Flux ;⧫:experiment

From results of Figure 7 and Figure 8 we can conclude that the flame length is better predicted by the model R_{ij}-Flux. This model also predicts rather well radial profiles of temperature especially far downstream of the recirculation zone. These results are due to the calculation of turbulent scalar flux by their transport equations, so that the scalar field and finally the presumed pdf are better calculated

Conclusion :

In this study we calculated the characteristics of methane diffusion flame behind a bluff body obstacle. The dynamic and scalar fields are calculated from their transport equations. The temperature and the chemical species are calculated by the presumed pdf method. Beta function is used. It is based on the first two moments of an inert scalar (its mean and variance). Three turbulence models namely k-ε model, R_{ij}-ε model and R_{ij}-Flux model were tested, and the following conclusions can be made:

- The recirculation zone length is under-predicted by the three models. Also the stagnation point location is well predicted by the three models. However only the R_{ij} – Flux model predict correctly de decay rate of the axial velocity.
- The anisotropy of the flow is predicted by R_{ij} - ε and R_{ij} – Flux models.
- The flame length is well predicted by the model R_{ij} – Flux model. Indeed with this model the turbulent scalar flux is calculated by its transport equation, which means that the scalar field is better calculated in the whole, and consequently the shape of a presumed pdf.

References

1. Popov P.P., Pope S.B., *Combustion and Flame,* 161 (2014) 3100
2. Gao N., Li Y., Bai H., *Procedia Engin.*, 126 (2015) 532
3. Krajnovic S., Minelli G., Basara B., *Appl. Math. And Comp.*, 272 (2016) 692
4. Elkhoury M., J. Wind *Eng. Ind. Aerodyn.*, 154 (2016) 10
5. Schefer R.W., Namazian M., Kelly J., *AIAA Journal,* 32, N 9 (1994) 1844.

6. Masri A.R., Dally B.B., Barlow R.S., Carter C.D., Twenty fifth Symposium (Intern.) on combustion (1994) 1301.
7. Ma H.K., Harn J.S., *Int J. Heat Mass Transfer,* 37, N 18 (1994) 2957.
8. Borghi R., Prog. Energy Com. Sci. 14 (1988) 245.
9. Monin A.S., *Izv. Akad.Nauk SSSR, Fiz.Atmos. Okeana,* 11 (1965) 45.
10. Beguier C., Dekeyser I., Launder B.E., *Physics of Fluids,* 21, N3 (1978) 307
11. Favre A, *Journal de Mécanique,* 4, N 3 (1965) 361
12. El amraoui R., Garreton D., rep. EDF-DER, HE. 44./95/014/A (1995).
13. Bel Hassan M., Simonin O., Fifth Intern. Symposium on refined Flow Modeling and Turbulence Measurements, in press de l'ENPC (eds), (1993) 537.
14. Bellil A, Benhabib K., Coorevits P., Marie C., Hazi M, Ould-Dris A., *J. Mater. Environ. Sci.* 6 (5) (2015) 1426
15. Rotta J.C., *Zeitschriftphy sic* 129 (1951) 547.
16. Naot D., Shavit A., Wolfshtein M., *Isr J. Tech.*, 8, N 3 (1970) 259.
17. Davidov B.I., *Dolk. Akad.Nauk., SSSR* 136 (1961) 47.
18. Harlow F.H., Nakayama P.I., Los Alamos Sci. Lab., Univ. of California, rep. LA-4086 (1968).
19. Hanjalic K., Launder B.E., *J. Fluid Mech.* 52 (1972) 609
20. Launder B.E., Reece G.J., Rodi W., *J. Fluid Mech.* 68 part 3 (1975) 537.
21. Hogg S., Leschziner M.A., *Int J. Heat Fluid Flow,* 10 N 1 (1989) 16.
22. Glassman I., ISBN 0-12-285851-4 (1987) Academic Press Inc. London
23. Attiti A., Bisetti F., Mueller M., Pitsch H., *Proc. Comb. Institute* 35 (2015) 1217
24. Sanchez – Sanz M., Fernandez – galisteo D., Kurdyumov V.N., *Comb. Flame,* 161 (2014) 1282
25. Prud'homme R., ISBN 978-0-8176-4518-2 (2010) Springer Science LLC 201
26 Bouvet N., Halter F., Chauveau Ch., Yoon Y., *Int. J. Hydrog. Energy* 38 (2013) 5949
27. Barlow R.S., Frank J.H., Karpetis A.N., Chen J.Y., *Comb. Flame* 143 (2005) 433
28. Attiti A., Bisetti F., Mueller M., Pitsch H., *Comb. Flame* 166 (2016) 192
29. Law C.K., ISBN – 13 978-0-511-24584-8 eboook (EBL) (2006) Cambridge Univ. Press
30. Spalding D.B., *Chem. Engn. Sc.* (1971) 26
31. Lockwood F.C., *combustion and flame,* 24 (1975) 109.
32. Rodes R.P., Harsha A.P.T., *AIAA Paper,* N 72.68 (1972).
33. Richardson J.M., Howard H.C., Smith R.W., Fourth Symposium on combustion, Williams and Wilkins (1953) 814.
34. Spalding D.B., Thirteenth Symposium (Inter.) on combustion (1971) 649.
35. Launder B.E., 1975, *J. Fluid Mech.* 67 (1975) 569.
36. Warhaft Z., Lumley J. L. , *J. Fluid Mech.* 88 (1978) 659.
37. Simonin O., BechardJ.,rep. EDF-DER-LNH, HE. 44./90.06 (1990).
38.Namazian M., Kelly J., Schefer R.W., Johnston S.C., Long M.B, Exp. in Fluids 8 (1989) 216.
39. Correa S.M., Gulati A., *combustion and flame* 89 (1992) 279.
40. Correa S.M., Pope S.B., Twenty four Symposium (Intern.) on combustion (1992) 1167.
41. Garreton D., Simonin O., rep. EDF-DER HE. 44./95/015/A (1995).
42. El amraoui R., 1993, PhDThesis, Université de Rouen